13—27

Estimating Light Position and Surface Reflectance from Specular Reflection under Perspective Projection

Kenji Hara* † Ko Nishino*‡ Atsushi Nakazawa* Katsushi Ikeuchi*

* Department of Computer Science
The University of Tokyo

Abstract

In this paper, we propose a new method for estimating reflection properties of a real object surface from a single specular component image, as well as the light source position. Polarization is used for separating the diffuse and specular reflection components. Different from previous approaches, which heavily assumed both distant viewpoint and illuminant position, our method can work even under short distance of them. Given a specular reflection component, the method begins with estimating the position of the light source. At the same time, the initial values of reflectance parameters are also estimated by linearizing the reflection model with a variable transformation. The estimated illuminant position and reflection parameters are then refined based on the original reflection model.

1 Introduction

Estimating the illumination of a real scene from a single image is an important issue in computer vision and augmented reality research. For example, augmented reality allows us to see the real world scene seamlessly with virtual objects superimposed on it. To generate a highly photo-realistic augmented image, the virtual object has to be shaded consistently under the real illumination condition of the other objects in the scene. Moreover, the realistic reflectance properties also have to be used for synthesizing the virtual object images with realistic shading effects. Therefore, it is desirable to solve the following two problems simultaneously: (1) estimating the illumination of a real scene from a single image; and (2) measuring the surface reflectance properties of a real object in the scene from a single image.

In the past, several techniques to estimate reflectance properties from a single image with known illumination have been developed. Those techniques first assume uniform reflectance properties over the object surface, and then generate a new synthetic image by using an iterative method that minimizes the error between the real and synthetic image with respect to the reflectance parameters [1, 2]. On the other hand, a few methods have been developed for estimating the illumination of a real scene from a single image by using the surface reflectance properties. I. Sato *et al.* [3] proposed a method for estimating the complex illumination distribution of a real scene by using a radiance distribution inside shadows cast by a real object.

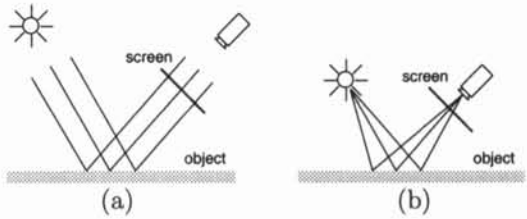

Figure 1: Illuminant and viewpoint assumptions.

However, few methods have been proposed for estimating reflection parameters of a real object surface from a single image, as well as the illuminant position. Ikeuchi *et al.* [3] developed an algorithm to determine both the surface reflectance properties and the light source direction from a single image based on analysis of a simplified Torrance-Sparrow reflection model [12]. Ramammorthi *et al.* [5] derived an equation in terms of spherical harmonic coefficients of the reflectance properties and illumination condition. Then, they deconvolved it for simultaneously recovering the illumination distribution and surface reflection properties. Tominaga *et al.* [6] adopted the Phong model to determine the surface reflectance properties and the direction of illumination from a single color image. However, the above techniques heavily assumed both distant illumination and viewpoint (see Fig 1(a)) and can not handle adequately real scenes under short distance of them. Our method aims at estimating reflection properties of a real object surface from a single image, as well as the light source position even under short distance of illumination and viewpoint (see Figure 1(b)).

We propose a two-stage iterative technique that minimizes the difference between the synthesized image and the real one, based on the variation of angle data due to perspective projection and nearby illumination. We use polarization for separating the diffuse and specular reflection components. Given a specular reflection component, the method begins with estimating the position of the light source. At the same time, the initial values of reflectance parameters are also estimated by linearizing the Torrance-Sparrow reflection model with a variable transformation. The estimated illuminant position and reflectance parameters are then refined based on the original reflection model. Some results of experiments using synthetic and real data are presented in the paper.

*Address: 4-6-1 Komaba, Meguro-ku, Tokyo Japan. E-mail: {hara,kon,nakazawa,ki}@cvl.iis.u-tokyo.ac.jp
†Fukuoka Prefectural Government Office in Tokyo
‡Columbia University

2 Polarization-Based Separation of Reflection Components

2.1 Reflection Mechanism

In general, reflection models are described by linear combinations of two reflection components: the diffuse reflection and the specular reflection. This physical model was formally introduced by Shafer [7] as the dichromatic reflection model. The diffuse reflection component represents the reflected rays arising from internal scattering inside surface medium. The light waves penetrate the surface, internally multiply refract, and then refract back out into air with a variety of directions.

The specular reflection component, on the other hand, represents the light rays reflected on the object surface. The surface may be assumed to be composed of microscopic planar elements, each of which has its own surface orientation different from the microscopic local orientation of the surface. The result is the specular reflection component that spreads around the specular direction and that depends on the surface roughness for the width of the distribution [8].

2.2 Polarization

In our appearance analysis, polarization is used for separating the diffuse and specular reflection components. Wolff et al. [8] have proposed an algorithm which analyzes linear polarization states of highlights removal and material classification. Boult et al. [9] have also studied the classification of scene edges based on their polarization characteristics. Recently, Miyazaki et al. [10] have proposed a method for obtaining surface orientations of transparent objects by analyzing the degree of polarization in visible and far-infrared wavelengths.

The separation method adopted in this paper uses two linear polarization filters [11]. One is placed in front of a point light source in order to polarize the light source linearly, and the other is placed in front of a camera to capture images through the linear polarization filter. For an ideal filter, a light wave should be passed unattenuated when its electric field is aligned with the polarization axis of the filter, and the energy is attenuated as a trigonometric function when the filter is rotated.

As described in the previous subsection, the image brightness value taken by sensor is described as

$$I = I_d + I_s \tag{1}$$

where I_d and I_s represent the diffuse and specular components, respectively.

When incident light is linearly polarized, the diffuse component tends to be unpolarized due to its internal scattering. In contrast, the specular reflection component tends to remain linearly polarized. Therefore, the observed brightness of the specular component can be expressed as a trigonometric function for polarization filter angle, and that of the diffuse component can be expressed as a constant. Thus, the image brightness observed through a linear polarization filter is described as

$$I = I_c + I_v(1 + \cos 2(\theta - \beta)) \tag{2}$$

where θ is the angle of the polarization filter and β is the phase angle determined by the projection of the surface normal onto the plane of the filter.

It should be noted that in the above equation I_c is not equal to the real diffuse intensity, and $2 \times I_v$ is not equal to the real specular intensity. Both of specular and diffuse components are attenuated traveling through the polarization filter and image brightness gets darker overall the object surface.

The polarization state of reflected light depends on several factors including the material of the reflecting surface element, and the type of reflection component, i.e. diffuse or specular. In order to describe the state of polarization of the reflected light, the Fresnel reflection coefficients $F_\perp(\eta, \psi)$ and $F_\parallel(\eta, \psi)$ are used [8]. The Fresnel reflection coefficients determine the polarization of reflected light waves in the directions perpendicular and parallel to the plane of incidence, respectively, and determine the maximum and the minimum intensities which are observed when the angle of the polarization filter varies. The parameter η is the complex index of refraction of the surface medium and the parameter η is the incident angle. Since we use a linearly polarized light source, we can assume that the intensity of the specular component observed through a linear polarization filter is guaranteed to become equal to zero at a certain angle. Hence, we obtain the following relation between I_v and specular reflection intensity:

$$q = \frac{F_\perp(\eta, \psi)}{F_\parallel(\eta, \psi)} \tag{3}$$

$$2I_v = \frac{q}{1+q} I_s \tag{4}$$

where I_s is the specular reflection intensity.

It is known that the diffuse component is also polarized when the viewing angle is close to 90 degrees, e.g., near the occluding contour of an object. However, the diffuse component becomes linearly polarized only in narrow region and the degree of polarization in the diffuse reflection component is generally negligible. Hence, we assume that the diffuse component is unpolarized in our analysis. The intensity of unpolarized light is attenuated by half when it passes a linear polarization filter. As a result, I_c and the diffuse component have a relation as

$$I_c = \frac{1}{2} I_d \tag{5}$$

where I_d is the diffuse reflection intensity.

2.3 Separation of Reflection Components

For separating the diffuse and specular reflection components, images of a target object are taken every certain degrees filter rotation. Then, the maximum intensity I_{max} and the minimum intensity I_{min} are determined for every image pixel. If $I_{max} - I_{min}$ for a certain pixel is less than a threshold, we consider the pixel to contain only the diffuse component. If $I_{max} - I_{min}$ is larger than a threshold value, we determine the pixel contains the specular component and the specular component intensity is obtained from $I_{max} - I_{min}$. I_{min} is used for determining the diffuse component intensity.

3 Illuminant Position and Reflectance Parameter Estimation

After separating the reflection components, we estimate the position of the single point light source, as well as the specular reflection parameters, using only the specular reflection component.

3.1 Reflection Model

In our system, we use the Torrance-Sparrow reflection model [12] simplified by assuming that the Fresnel reflectance coefficient is constant and the geometric attenuation factor is 1. With this reflection model, the specular reflection at a surface point is given as

$$E_{s,m} = \frac{I_{s,m}}{L_m} = \frac{K_{s,m}}{\cos\theta_r} \exp\left[-\frac{\alpha^2}{2\sigma^2}\right] \tag{6}$$

where m stands for each R, G and B component, $I_{s,m}$ is the specular component intensity, θ_r is the angle between the viewing direction and the surface normal, α is the angle between the surface normal and the bisector of the viewing direction and the light source direction, $K_{s,m}$ is a constant for the specular reflection component, and σ is the surface roughness measured as the standard deviation of microfacet slope. L_m is the irradiance given by

$$L_m = \frac{L_{q,m}}{r^2} \tag{7}$$

where $L_{q,m}$ is the luminous power and r is the distance between the point light source and the surface point.

In the original Torrance-Sparrow reflection model, the coefficient $K_{s,m}$ contains the Fresnel reflectance coefficient and the geometric attenuation factor. In order to handle this $K_{s,m}$ as a constant, we assume that the viewing angle θ_r and the illuminating angle θ_i are less than 60° [13]. Moreover, note the angle θ_r can be computed at each image pixel by range scanning and camera calibration, and the angle α can be expressed as a function of the illuminant position $\boldsymbol{L}$ as $\alpha = \alpha(\boldsymbol{L})$ and thus its value is now unknown.

In this paper, we refer to ($\bar{K}_s = [K_{s,R}, K_{s,G}, K_{s,B}]^T$ and σ) as the specular reflection parameters.

3.2 Illuminant Distance

We can compute the illuminant direction at the object surface point P satisfying $\theta_i = \theta_r$, i.e., $\alpha = 0$ as

$$\boldsymbol{L}_p = \boldsymbol{N}_p + (\boldsymbol{N}_p, \boldsymbol{V}_p)\boldsymbol{N}_p - \boldsymbol{V}_p \tag{8}$$

where $\boldsymbol{L}_p$ is the unit vector to represent the illuminant direction. $\boldsymbol{N}_p$ and $\boldsymbol{V}_p$ are the unit vectors to represent the surface normal and viewing direction, respectively. Using $\boldsymbol{L}_p$, we can express the illuminant position $\boldsymbol{L}$ as

$$\boldsymbol{L} = \boldsymbol{P} + t\boldsymbol{L}_p \tag{9}$$

where $\boldsymbol{P}$ is the location vector of P and t is the distance between $\boldsymbol{P}$ and $\boldsymbol{L}$.

The surface point P corresponds to the peak pixel location (x_p, y_p). Once we get (x_p, y_p), $\boldsymbol{P}$ can be calculated using the camera projection matrix, and hence $\boldsymbol{L}_p$ can be also computed from equation (8). As a result, only t is unknown and needs to be determined for estimating illuminant position. From now on, we refer to t as the illuminant distance. On the other hand, for estimating the specular reflection parameters, $K_{s,R}$, $K_{s,G}$, $K_{s,B}$, and σ have to be determined.

3.3 Initial Estimation

The analysis approach described in the last section is too sensitive to noise. In the following description, from a practical viewpoint, we explain how to determine the illuminant position $\boldsymbol{L} = (x_l, y_l, z_l)^T$ from the single specular image.

The following equation can be derived by the logarithm transformation of equation (6):

$$\ln E_{s,m} = \ln K_{s,m} - \frac{\alpha^2}{2\sigma^2} - \ln\cos\theta_r. \tag{10}$$

Thus, we obtain the linearized reflection model as

$$Y_m = -\frac{1}{\sigma^2}X + \ln K_{s,m} \tag{11}$$

where

$$X = \frac{\alpha^2}{2} = \frac{\alpha(t)^2}{2}, \tag{12}$$

$$Y_m = \ln E_{s,m} + \ln\cos\theta_r. \tag{13}$$

Our basic idea is to find $\boldsymbol{L}$ that generates 2D points in the parameter space (X, Y_m), $\{(X_j, Y_{mj})\}$, which a line best fits. To define the objective function for this optimization, we use a statistical evaluation called the correlation coefficient as follows.

The correlation coefficient measures linear relationship between two variables. Given N 2D points $\{(x_i, y_i)\}$ $(i = 1, 2, \cdots, N)$, the correlation coefficient r_{xy} is defined by

$$r_{xy} = \frac{\sum(x_i - \overline{x})(y_i - \overline{y})}{\sqrt{\sum(x_i - \overline{x})^2}\sqrt{\sum(y_i - \overline{y})^2}} \tag{14}$$

where $\sum$ stands for the sum from $i = 1$ to $i = N$, and $\overline{x}$ and $\overline{y}$ are the mean values satisfying $\sum_{i=1}^{N} x_i = N\overline{x}$ and $\sum_{i=1}^{N} y_i = N\overline{y}$, respectively. The value of r_{xy} can range from -1 to $+1$. If there is no linear relationship between x and y, r_{xy} is 0. If there is a perfect positive (negative) relationship, r_{xy} is $+1$ (-1). Therefore, since the slope of equation (11) is always negative, we define the objective function to be minimized with regard to $\boldsymbol{L}$ as

$$E_p(x_p, y_p, l_p) = r_{XY_R} + r_{XY_G} + r_{XY_B} \tag{15}$$

where r_{XY_m} is the correlation coefficient between the variables X and Y_m in equation (12) and (13) for $m = R, G, B$.

Since the minimization of E_p is difficult to carry out analytically, we get the solution by searching a discrete parameter space. We search the illuminant distance t which minimizes $E_p(t)$ by discretizing t with steplength $\Delta_t = 1\,\text{mm}$, within $0 < t \leq t_{max}$, where t_{max} is the user-defined upper bound of t. From the resultant t^*, the optimal position $\boldsymbol{L}^*$ can be calculated.

Once we obtain $\boldsymbol{L}^*$, from equation (12) and (13), we can plot 2D points $\{(X_j, Y_{mj})\}$. After that, by first fitting a line to these 2D points via a least-squares method and then comparing the regression line with

equation (11), the estimates of the specular reflection parameters, $(\tilde{K}_s^*, \sigma^*)$, can be given as

$$K_{s,m}^* = \exp(b_m) \tag{16}$$

$$\sigma_m^* = \sqrt{-\frac{1}{a_m}} \tag{17}$$

where $a_m < 0$ and b_m are, respectively, the slope and Y-intercept of the least-squares regression line for the 2D points $\{(X_j, Y_{mj})\}$ for $m = R, G, B$. However, though the surface roughness is independent of three color channels, the above σ_R^*, σ_G^*, and σ_B^* often have the different values due to noise. Thus, we finally define the estimate of the roughness, σ^*, by the mean of σ_R^*, σ_G^*, and σ_B^*.

3.4 Refinement

Since the specular reflection parameter estimation in the last section is based on the logarithm fitting, the image synthesized based on the estimates $(\tilde{K}_s^*, \sigma^*, t^*)$ is still too different from the observed image. In this section, we refine $(\tilde{K}_s^*, \sigma^*, t^*)$ by solving a nonlinear optimization problem based on the original reflection model given in equation (6).

Now, suppose we have N_k surface points of the target object in the image, the error between the input specular image and the model-based rendering image is evaluated by

$$E_{nergy}(\tilde{K}_s, \sigma, t) = \sum_{m\in\{R,G,B\}} \sum_{k=1}^{N_k} \left(E_s^{(k)} - \frac{K_{s,m}}{\cos(\theta_r^{(k)})} \times \exp\left[-\frac{(\alpha^{(k)}(t))^2}{2\sigma^2}\right] \right)^2 \tag{18}$$

where $E_s^{(k)}$ and $(\theta_r^{(k)}, \alpha^{(k)})$ are, respectively, the ratio E and the angles (θ_r, α) measured at the kth surface point in the input specular image. Minimizing equation (18) locally around the initial guesses $(\tilde{K}_s^*, \sigma^*, t^*)$ via the Alternating Minimization (AM) algorithm [14], we can obtain the final estimation of the reflection parameters, $(\tilde{K}_s^{**}, \sigma^{**}, t^{**})$. The procedure is described in the following.

1. Set n=0, $\tilde{K}_s^{(0)} = \tilde{K}_s^*$, $\sigma^{(0)} = \sigma^*$, and $t^{(0)} = t^*$
2. Update $\tilde{K}_s^{(n)}$ for fixed $\sigma^{(n)}$ and $t^{(n)}$as

$$K_{s,m}^{(n+1)} = \sum_{k=1}^{N_k} E_{s,m}^{(k)} \Big/ \sum_{k=1}^{N_k} \frac{1}{\cos(\theta_r^{(k)})} \exp\left[-\frac{\alpha^{(k)}(t^{(n)})^2}{2(\sigma^{(n)})^2}\right] \quad m = R, G, B$$

3. Set $n' = 0$ and $\sigma^{(0)} = \sigma^{(n)}$
4. Update $\sigma^{(n')}$ for fixed $\tilde{K}_s^{(n+1)}$ and $t^{(n)}$ as

$$(4-1)\quad \kappa^{(n')} = \frac{1}{\sigma^{(n')}}$$

$$(4-2)\quad \kappa^{(n'+1)} = \kappa^{(n')} - \gamma \sum_{m\in\{R,G,B\}} \sum_{k=1}^{N_k} \left(I_s^{(k)} - \frac{K_{s,m}^{(n+1)}}{\cos(\theta_r^{(k)})} \exp\left[-\frac{(\alpha^{(k)}(t^{(n)}))^2(\kappa^{(n)})^2}{2}\right] \right)^2 \times \frac{K_{s,m}^{(n+1)}(\alpha^{(k)}(t^{(n)}))^2\kappa^{(n)}}{\cos(\theta_r^{(k)})} \exp\left[-\frac{(\alpha^{(k)}(t^*))^2(\kappa^{(n)})^2}{2}\right]$$

$$(4-3)\quad \sigma^{(n'+1)} = \frac{1}{\kappa^{(n'+1)}}$$

5. If $|\sigma^{(n'+1)} - \sigma^{(n')}| > \epsilon_1$, set $n' \leftarrow n' + 1$ and go to 4. Otherwise set $\sigma^{(n+1)} = \sigma^{(n'+1)}$
6. Update $t^{(n)}$ for fixed $\tilde{K}_s^{(n+1)}$ and $\sigma^{(n+1)}$ as

$$t^{(n+1)} = \arg\min_{t\in T^{(n)}} E_{nergy}(\tilde{K}_s^{(n+1)}, \sigma^{(n+1)}, t)$$

where $T^{(n)} = \{t^{(n)} - \Delta t, t^{(n)}, t^{(n)} + \Delta t\}$

6. If $|K_{s,m}^{(n+1)} - K_{s,m}^{(n)}| > \epsilon_2$ or $|\sigma^{(n+1)} - \sigma^{(n)}| > \epsilon_3$ or $|t^{(n+1)} - t^{(n)}| > \epsilon_4$, set $n \leftarrow n + 1$ and go to 2.

In the above procedure, n and n' are time steps, $\epsilon_1 \sim \epsilon_4$ are thresholds, γ is a positive number for the steepest descent method, and Δt is a positive number. We show the outline of the overall algorithm in Fig.2.

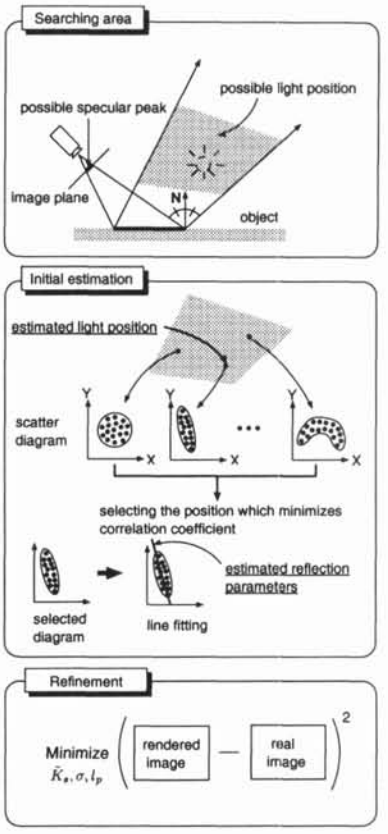

Figure 2: Basic steps of the proposed method.

4 Experiments

In this section, we present results of two experiments using synthesized and real images. The first experiment using synthesized images is made mainly to show

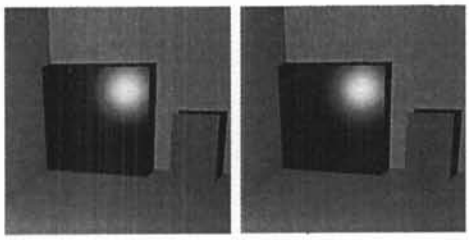

(a) (b)

Figure 3: Synthesized image: (a)input image, (b)synthesized image.

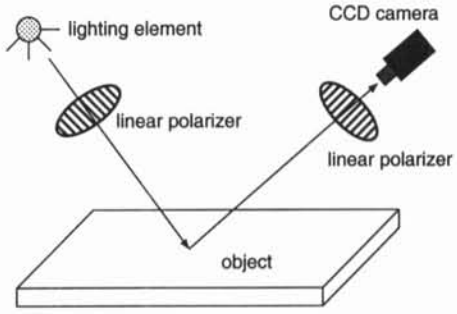

Figure 4: Experimental setup.

the capacity of our method in estimating illuminant positions accurately. The second experiment using real images aims to examine the applicability of our method to real problems.

4.1 Experiment Using Synthesized Image

Fig.3(a) shows the original synthetic specular image generated using a well-known rendering software called RADIANCE [15]. The object to be modeled in this experiment is a large board in the center of the image. RADIANCE employs an empirical reflection model proposed by Ward [16] as follows.

$$E_s = \frac{\rho_s}{\sqrt{\cos\theta_i \cos\theta_r}} \frac{\exp[-\tan^2\alpha/\sigma'^2]}{4\pi\sigma'^2} \quad (19)$$

where θ_i, θ_r, and α are all the same as those of Torrance-Sparrow reflection model, ρ_s is the specular reflectance, σ' is the surface roughness. Since Ward's model parameters (ρ_s, σ') can not be simply compared with Torrance-Sparrow model parameters (K_s, σ), we examine only the illuminant position estimation of our method. After the first-stage initial estimation, we obtain $\boldsymbol{L}^* = [11.81, 2.16, 3.051]$ to the true value $\boldsymbol{L}_{true} = (13, 2, 3)$. After the final-stage refinement, we obtain $\sigma^{**} = 0.057$ and $\tilde{K}_s^{**} = [0.84, 0.85, 0.84]^T$. Fig.3(b) illustrates the image rendered by using $\boldsymbol{L}^*$, σ^{**}, and $\tilde{K}_s^{**}$.

4.2 Image Acquisition System

In this section, we explain the experimental setup used in the second experiment (Fig.4), which is described in the next section. A range image is obtained using a light-stripe range finder with a liquid crystal shutter and a color CCD video camera. Each range image pixel represents an 3-D location of a corresponding point on an object surface. The same color camera is used for acquiring range images and color images. Color images are taken through a polarization filter.

A halogen lamp is used as a light source. The lamp is small enough for us to assume the lamp is a point light source. In order to illuminate the object with linearly polarized illuminant, a linear polarization filter is placed in front of the lamp.

4.3 Experiment Using Real Image

Fig.5(a) shows the original real image. The object to be modeled is a blue bookend in this scene. Fig.5(b) and (c) show the diffuse and specular reflection components separated by using polarization filters, respectively. The image shown in Fig.5(c) is used as input to our estimation method.

After the first-stage initial estimation, we get $\boldsymbol{L}^* = (-9.89, 6.95, 15.62)^T$. Finally, we obtain $\sigma^{**} = 0.079$ and $\tilde{K}_s^{**} = [0.29, 0.40, 0.34]^T$. Fig.6(a) illustrates the specular synthetic image recovered by using $\boldsymbol{L}^*$, σ^{**}, and $\tilde{K}_s^{**}$. Fig.6(b) shows the final synthetic image generated by composing the synthetic specular image (Fig.6(a)) and the real diffuse image (Fig.5(b)).

Finally, we demonstrate the results of running our algorithm on a curved surface object. Fig.7(a) shows the original real image. Fig.7(b) and Fig.7(b) show, respectively, the diffuse and specular components separated by using polarization. Fig.7(d) shows the result of adding the synthesized specular image to the diffuse component shown in Fig.7(b).

5 Conclusion

In this paper, we have proposed a new method that estimates the reflectance properties of the object surface as well as the illuminant position even under nearby viewpoint and illumination. The input data are a 3D geometric model of the target object and a single specular component image separated using polarization filter. By using a two-stage iterative algorithm, the specular parameters of Torrance-Sparrow reflection model and 3D position of the single point light source are determined simultaneously. We have shown that the method can be successfully used for producing photo-realistic synthetic object images under unknown illumininant positions.

References

[1] A. Fournier, A. Gunawan, and C. Romanzin, "Common illumination between real and computer generated scenes," *Proc. Graphics Interface '93*, pp.254-262, 1993.

[2] S. Boivin and A. Gagalowicz, "Image-based rendering of diffuse, Specular and Glossy Surfaces from a single image," *Computer Graphics Proceedings, SIGGRAPH2001*, pp.107-116, 2001.

[3] I. Sato, Y. Sato, and K. Ikeuchi, "Ilumination distribution from shadows," *Proceedings of IEEE Conference on Computer Vision and Pattern Recognition*, pp.306-312, 1999.

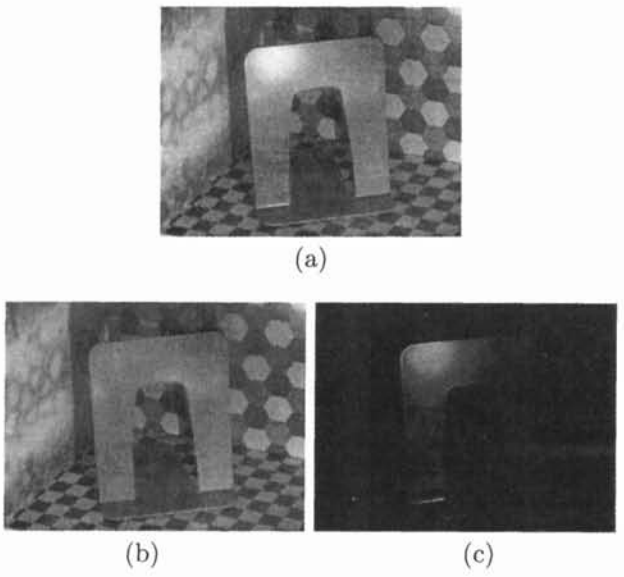

Figure 5: Separation of reflection components: (a)original image, (b)separated diffuse component, (c)separated specular component.

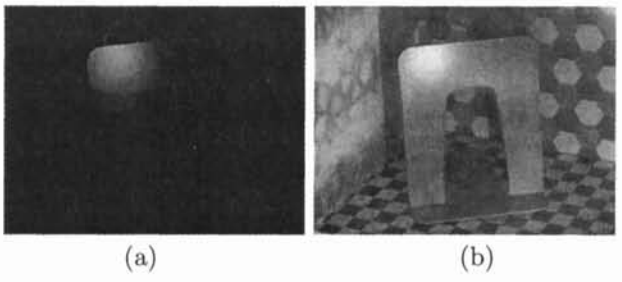

Figure 6: Synthesized image: (a)synthesized specular image, (b)synthesized image.

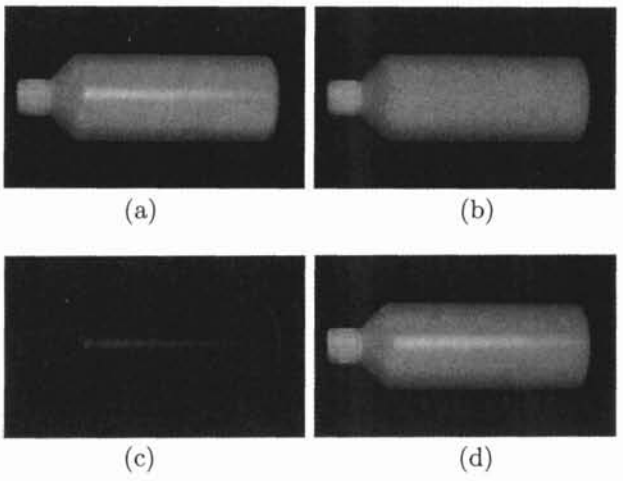

Figure 7: Curved object: (a)input image, (b)separated diffuse component, (c)separated specular component, (d)synthesized image.

[4] K. Ikeuchi and K. Sato, "Determining reflectance properties of an object using range and brightness images," *IEEE Trans. Pattern Analysis and Machine Intelligence*, Vol.13, No.11, pp.1139-1153, 1991.

[5] R. Ramamoorthi and P. Hanrahan, "A signal processing framework for inverse rendering," *Computer Graphics Proceedings, SIGGRAPH2000*, pp.379-387, 2000.

[6] Tominaga, S. and Tanaka, N.: Estimating reflection parameters from a single color image, *IEEE Computer Graphics and Applications*, Vol.20, No.5, pp.58-66 (2000).

[7] S. Shafer, "Using color to separate reflection components," *COLOR Research and Application*, Vol. 10, pp. 210-218, 1985.

[8] Wolff, L.B. and Boult, T.E.: Constraining object features using a polarization reflectance model, *IEEE Trans. Pattern Analysis and Machine Intelligence*, Vol.13, No.6, pp.167-189 (1991).

[9] Boult, T.E. and Wolff, L.B. : Phisically based edge labeling, *Proceedings of Computer Vision and Pattern Recogition*, pp.656-663 (1991).

[10] D. Miyazaki, M. Saito, Y. Sato, and K. Ikeuchi, "Determining surface orientations of transparent objects based on polarization degrees in visible and infrared wavelengths," *Journal of the Optical Society of America*, Vol.19, pp.687-694, 2002.

[11] T. Takahashi, Y. Sato, and K. Ikeuchi, "Separating the reflection components with the use of polarization and determining the reflection parameters," *IPSJ CVIM*, Vol.2000, 2000.

[12] Torrance, K.E. and Sparrow, E.M.: Theory of off-specular reflection from roughened surfaces, *Journal of the Optical Society of America*, Vol.57, pp.1105-1114 (1967).

[13] Nayar, S.K., Ikeuchi, K. and Kanade, T.: Surface reflection: physical and geometrical perspectives, *IEEE Trans. Pattern Analysis and Machine Intelligence*, Vol.13, No.7, pp.611-634 (1991).

[14] Chan, T.F. and Wong, C.K.: Convergence of the alternating minimization algorithm for blind deconvolution, *Linear Algebra and its Applications*, Vol.316, 1-3, Sep 2000, pp.259-285 (2000).

[15] http://radsite.lbl.gov/radiance/HOME.html

[16] Ward, G.J.: Measuring and modeling anisotropic reflection, *Computer Graphics Proceedings, SIGGRAPH2000*, pp.265-272 (1992).